J|A|C|S ARTICLES

Published on Web 07/15/2010

'Carbene Radicals' in Co^{II}(por)-Catalyzed Olefin Cyclopropanation

Wojciech I. Dzik,[†] Xue Xu,[‡] X. Peter Zhang,[‡,*] Joost N. H. Reek,[†] and Bas de Bruin[†,*]

Department of Homogeneous and Supramolecular Catalysis, Van't Hoff Institute for Molecular Sciences (HIMS), University of Amsterdam, Nieuwe Achtergracht 166, 1018 WV Amsterdam, the Netherlands, and Department of Chemistry, University of South Florida, Tampa, Florida 33620

Received May 3, 2010; E-mail: b.debruin@uva.nl; xpzhang@usf.edu

Abstract: The mechanism of cobalt(II)−porphyrin-mediated cyclopropanation of olefins with diazoesters was studied. The first step—reaction of cobalt(II)−porphyrin with ethyl diazoacetate (EDA)—was examined using EPR and ESI-MS techniques. EDA reacts with cobalt(II)−porphyrin to form a 1:1 Co(por)(CHCOOEt) adduct that exists as two isomers: the 'bridging carbene' **C′** in which the 'carbene' is bound to the metal and the pyrrolic nitrogen of the porphyrin that has a d^7 configuration on the metal, and the 'terminal carbene' **C** in which the 'carbene' behaves as a redox noninnocent ligand having a d^6 cobalt center and the unpaired electron residing on the 'carbene' carbon atom. The subsequent reactivities of the thus formed 'cobalt carbene radical' with propene, styrene, and methyl acrylate were studied using DFT calculations. The calculations suggest that the formation of the carbene is the rate-limiting step for the unfunctionalized Co^{II}(por) and that the cyclopropane ring formation proceeds via a stepwise radical process: Radical addition of the 'carbene radical' **C** to the C=C double bonds of the olefins results in formation of the γ-alkyl radical intermediates **D**. Species **D** then easily collapse in almost barrierless ring-closure reactions (**TS3**) to form the cyclopropanes. This radical mechanism readily explains the high activity of Co^{II}(por) species in the cyclopropanation of electron-deficient olefins such as methyl acrylate.

1. Introduction

Transition metal-catalyzed olefin cyclopropanation with diazo reagents is one of the most attractive methods to prepare functionalized cyclopropanes, which have found a myriad of fundamental and practical applications. Highly diastereo- and enantioselective catalytic systems, which are mainly based on diamagnetic Cu^I and binuclear Rh_2 paddlewheel complexes, have been successfully developed to catalyze certain types of cyclopropanation reactions.[1] While excellent results with styrenes and other electron-rich olefins have been obtained with these catalysts, their performance with electron-deficient olefins (e.g., acrylates) is, however, problematic due to the electrophilic nature of the metal−carbene intermediate.

Since the discovery that cobalt(II) complexes are capable of (stereo- and enantioselective) olefin cyclopropanation reactions,[2] various cobalt-based catalytic systems have been developed. So far, the most successful cobalt-based catalysts are complexes with salen[3] and porphyrin[4] ligands developed by the groups of Katsuki and Zhang, respectively. Chiral cobalt−porphyrin cyclopropanation catalysts are unprecedented in their reactivity, stereocontrol, and ability to affect cyclopropanation with (near) stoichiometric amounts of alkenes avoiding carbene dimer formation.[5] Another intriguing feature of the cobalt(II) porphyrin systems is their effectiveness in cyclopropanation of electron-deficient olefins, such as methyl acrylate or acrylonitrile, while they perform rather poorly in the cyclopropanation of aliphatic alkenes (Scheme 1).[4d,f] This reactivity is remarkable

Scheme 1. Cobalt(II)−Porphyrin-Catalyzed Cyclopropanation of Electron-Deficient Olefins

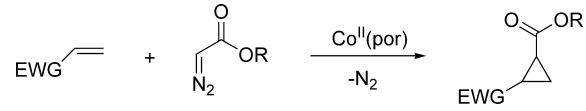

[†] Van't Hoff Institute for Molecular Sciences (HIMS), University of Amsterdam.

[‡] University of South Florida.

(1) For reviews on this topic see, for instance: (a) Doyle, M. P.; Forbes, D. C. *Chem. Rev.* **1998**, *98*, 911–935. (b) Kirmse, W. *Angew. Chem., Int. Ed.* **2003**, *42*, 1088–1093. (c) Wee, A. G. H. *Curr. Org. Synth.* **2006**, *3*, 499–555. (d) Davies, H. M. L.; Hedley, S. J. *Chem. Soc. Rev.* **2007**, *36*, 1109–1119.

(2) (a) Nakamura, A.; Konishi, A.; Tatsuno, Y.; Otsuka, S. *J. Am. Chem. Soc.* **1978**, *100*, 3443–3448. (b) Nakamura, A.; Konishi, A.; Tsujitani, R.; Kudo, M.; Otsuka, S. *J. Am. Chem. Soc.* **1978**, *100*, 3449–3461.

(3) (a) Niimi, T.; Uchida, T.; Irie, R.; Katsuki, T. *Tetrahedron Lett.* **2000**, *41*, 3647–3651. (b) Niimi, T.; Uchida, T.; Irie, R.; Katsuki, T. *Adv. Synth. Catal.* **2001**, *33*, 79–88.

(4) (a) Huang, L.; Chen, Y.; Gao, G.-Y.; Zhang, X. P. *J. Org. Chem.* **2003**, *68*, 8179–8184. (b) Chen, Y.; Fields, K. B.; Zhang, X. P. *J. Am. Chem. Soc.* **2004**, *126*, 14718–14719. (c) Chen, Y.; Zhang, X. P. *J. Org. Chem.* **2007**, *72*, 5931–5934. (d) Chen, Y.; Ruppel, J. V.; Zhang, X. P. *J. Am. Chem. Soc.* **2007**, *129*, 12074–12075. (e) Zhu, S.; Ruppel, J. V.; Lu, H.; Wojtas, L.; Zhang, X. P. *J. Am. Chem. Soc.* **2008**, *130*, 5042–5043. (f) Zhu, S.; Perman, J. A.; Zhang, X. P. *Angew. Chem., Int. Ed.* **2008**, *7*, 8460–8463. (g) Ruppel, J. V.; Gauthier, T. J.; Snyder, N. L.; Perman, J. A.; Zhang, X. P. *Org. Lett.* **2009**, *11*, 2273–2276.

(5) For a highlight on the topic see: Doyle, M. P. *Angew. Chem., Int. Ed.* **2009**, *48*, 850–852.

and suggests some nucleophilic character of the carbene transfer intermediate in these reactions. This is unexpected, because in analogy with Cu- and Rh-based systems one would expect the formation of electrophilic (Fischer-type) transition-metal carbene intermediates from diazoesters with relatively late transition metals such as cobalt. This points to a very different character of the carbene transfer intermediate for Co^{II}(por)-based systems compared to the generic late transition metal electrophilic (Fischer-type) carbene intermediate.

Understanding these reactions in terms of a detailed reaction mechanism, thus explaining the above-mentioned unique reactivities and exceptional selectivities, will be important for future developments in (stereo)selective cyclopropanation reactions, especially regarding the use of diazo compounds (such as diazomalonates and diazoacetoacetates) and alkene substrates with which high selectivities have not yet been achieved. Detailed mechanistic insights in these reactions may well eventually allow us to expand the scope to other Co^{II}(por)-mediated ring-closing reactions (e.g., formation of five-membered rings from dienes and carbenes).

The available mechanistic information so far from previously reported kinetic studies and spectroscopic investigations using Co^{II}(salen) and Co^{II}(por) systems is fragmented and susceptible to different mechanistic interpretations. Reported DFT studies are restricted to information about simplified models of Co^{II}-(salen) systems and provide only limited information about small substrate models (ethene and diazoacetaldehyde).[6] As a result, questions regarding the (electronic) structures of the proposed cobalt carbene intermediates and transition states, as well as an estimate of the energy barriers on the basis of computational studies with realistic models, are unanswered. Especially, a rationale behind the remarkable activity of Co^{II}(por) systems toward *electron-deficient olefins* is an important question to answer. Clearly, the mechanism of Co^{II}-catalyzed cyclopropanation is poorly understood and requires detailed attention.[5]

Here we address the above questions in a combined experimental and computational approach. EPR spectroscopic studies and complementary DFT-EPR-property calculations allowed us to detect and characterize the elusive carbene-transfer intermediate operating in Co^{II}(por) systems, providing valuable new information about its unusual (electronic) structure. In addition, we performed a full mechanistic DFT study of the Co^{II}(por)-catalyzed cyclopropanation of methyl acrylate, styrene, and propene with methyl diazoacetate.

However, before we describe the details of our studies, let us first summarize the most relevant experimental mechanistic information available from previous reports in the next section (section 1.1).

1.1. Background and Available Experimental Mechanistic Information. Some kinetic and spectroscopic investigations of Co^{II}(TPP) (TPP = tetraphenylporphyrin)-catalyzed styrene cyclopropanation by ethyl diazoacetate (EDA) have been reported by Cenini and co-workers.[7] This system performed relatively well in the cyclopropanation of styrenes, while its reactivity toward relatively electron-rich aliphatic alkenes was rather poor. The kinetic studies revealed a first-order rate dependence on [catalyst], [EDA] and [styrene][8] concentrations.[9] The authors claimed the IR and NMR observation of a relatively stable 'carbene' species Co^{II}(TPP)(CHCOOEt), formed upon addition of EDA to Co^{II}(TPP), in which the :CHCOOEt moiety ends up bridging between the metal and a pyrrole nitrogen atom.[7] In general, carbene moieties can bind to transition metal porphyrin complexes in two ways: (1) classic coordination of the carbene carbon solely to the transition metal, where this 'terminal carbene' is generally thought to result in a metal−carbon double bond; and (2) as a 'bridging carbene' between the metal and a pyrrolato nitrogen of the porphyrin moiety, formed by insertion of the 'terminal carbene' into the M−N bond (see Figure 1).[10−15]

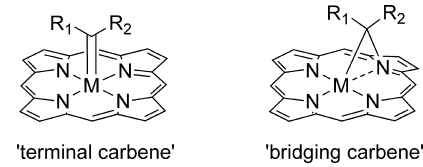

Figure 1. Possible coordination modes of carbenes to transition metal−porphyrin complexes.

The IR detection of the 'carbene' species, Co^{II}(TPP)-(CHCOOEt) was independently reported by Yamada and co-workers[16] although with a different carbonyl stretch frequency (ν_{CO} = 1597 cm^{-1} in DCM) than the one reported by Cenini and co-workers[7] (ν_{CO} = 1722 cm^{-1} in benzene). Yamada and co-workers assigned the IR signals to a 'terminal carbene'

(6) According to these DFT calculations with small models of the actual catalysts and substrates, strictly planar models seem to cyclopropanate ethene via a concerted carbene transfer mechanism from discrete Co^{II}-carbene intermediates to the olefin, but more flexible analogues prefer a pathway via a four-membered metallacyclic intermediate. In their earlier studies,[6a] the same authors described the possibility of a radical pathway involving 5-coordinate Co^{II}(salen)(L) for cyclopropanation with Co^{II}(salen) species in the presence of an axially coordinating neutral ligand L: (a) Ikeno, T.; Iwakura, I.; Yabushita, S.; Yamada, T. *Org. Lett.* **2002**, *4*, 517–520. (b) Iwakura, I.; Ikeno, T.; Yamada, T. *Org. Lett.* **2004**, *6*, 949–952.

(7) Penoni, A.; Wanke, R.; Tollari, S.; Gallo, E.; Musella, D.; Ragaini, F.; Demartin, F.; Cenini, S. *Eur. J. Inorg. Chem.* **2003**, 1452–1460.

(8) The order in [styrene] is somewhat more complex. A bell-shaped rate dependence on [styrene] was observed pointing to a first-order dependence at low styrene concentrations. The decreased rates at higher styrene concentrations were ascribed to substrate inhibition kinetics by the authors, but catalyst poisoning by an impurity (e.g. the stabilizer in styrene) cannot be excluded since the authors may have used non-purified styrene samples. For further discussion see the supporting information.

(9) The same group recently reported first-order kinetics in [catalyst] and [EDA], but zero order in [styrene] for related Co^{II}(salen) systems, suggesting that for these systems the energy barrier for the cyclopropanation step is considerably lower than that for the formation of the active carbene-transfer intermediate: Caselli, A.; Buonomenna, M. G.; de Baldironi, F.; Laera, L.; Fantauzzi, S.; Ragaini, F.; Gallo, E.; Golemme, G.; Cenini, S.; Drioli, E. *J. Mol. Catal. A.: Chem.* **2010**, *317*, 72–80.

(10) For a discussion on the possible binding modes and the factors that determine them see: Tatsumi, K.; Hoffmann, R. *Inorg. Chem.* **1981**, *20*, 3771–3784.

(11) Reactions of diazoesters with Co^{III}(por) complexes were extensively studied by the group of Johnson.[12] Most notably the reactions exclusively led to formation of 'bridging carbene' species, where the carbene ended-up bridging between cobalt and one of the pyrrolato nitrogen atoms of the porphyrin ring.[12] Also a bridging bis-carbene adduct was characterized crystallographically.[12d] Terminal carbene species could not be isolated. Recent investigations on reactions of diazoacetates with Co^{III}(salen) complexes suggest that also in this system a bridging carbene is preferred over a terminal carbene.[13]

(12) (a) Batten, P.; Hamilton, A.; Johnson, A. W.; Shelton, G.; Ward, D. *J. Chem. Soc., Chem. Comm.* **1974**, 550–551. (b) Johnson, A. W.; Ward, D.; Batten, P.; Hamilton, A. L.; Shelton, G.; Elson, C. M. *J. Chem. Soc., Perkin Trans. I* **1975**, 2076–2085. (c) Johnson, A. W.; Ward, D. *J. Chem. Soc., Perkin Trans. I* **1977**, 720–723. (d) Batten, P.; Hamilton, A. L.; Johnson, A. W.; Mehendran, M.; Ward, D.; King, T. J. *J. Chem. Soc., Perkin Trans. I* **1977**, 1623–1628.

(13) Koehn, S. K.; Gronert, S.; Aldajaei, J. T. *Org. Lett.* **2010**, *12*, 676–679.

Scheme 2. Redox Noninnocent Behavior of Carbene Ligands in Open-Shell d^7 Group 8 Transition Metal Complexes

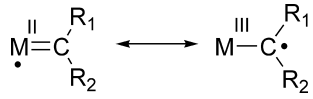

species, albeit with a cobalt−carbon single bond and proposed that this species has substantial unpaired spin density delocalized over the carbene carbon and its neighboring carbonyl moiety, in analogy with the 'terminal carbene' species proposed to be formed from Co^{II}(salen) and methyl diazoacetate (based on IR spectroscopy and complementary DFT calculations).[17] A similar mechanism was proposed by Zhang and co-workers in their original report on the discovery of Co^{II}(por)-catalyzed olefin cyclopropanation.[4a] For Ir^{II} complexes, de Bruin and co-workers recently demonstrated experimentally and computationally that carbene ligands generated from diazoesters like EDA at low-spin open-shell d^7 group 8 transition metals[18] indeed behave as so-called 'redox noninnocent' ligands.[19,20] In analogy, the elusive 'terminal carbene' Co^{II}(por)(CHCOOEt) species are perhaps not true 'carbenes' in the classic sense, but rather carbon centered 'carbene radicals' (see Scheme 2). This clearly adds to the complexity of our understanding of the (electronic) structure of 'carbene' intermediates in Co^{II}(por)-mediated cyclopropanation reactions (*vide infra*).

The proposed Co^{II}(por)(CHCOOEt) 'carbene' species could not be isolated because a fast reaction with additional EDA immediately produced diethyl maleate and (at higher EDA concentrations) the catalytically inactive diamagnetic species Co^{III}(TPP)(CH_2COOEt).[7] The latter species was characterized by X-ray diffraction and must be formed from Co^{II}(TPP)(CHCOOEt) by hydrogen atom abstraction from EDA or the solvent, indeed pointing to a significant radical character of the 'carbene' species. In the presence of styrene, no intermediates could be detected at all, and EDA dimerization was suppressed. Addition of the radical scavenger TEMPO (TEMPO = 2,2,6,6-tetramethylpiperidine *N*-oxide) substantially slowed down the cyclopropanation reaction, but no irreversible reaction occurred between Co^{II}(TPP) and TEMPO.[7,21−23] Hence, an intermediate with substantial unpaired spin density at one of the organic moieties must play an important role in the mechanism.

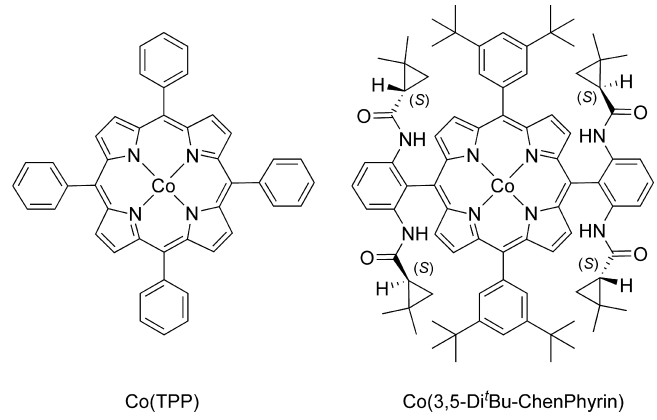

Figure 2. Cobalt(II) porphyrin complexes used in this study.

2. Results and Discussion

2.1. EPR Spectroscopy and ESI-MS Spectrometry. We decided to study the reaction of Co^{II}(por) species with ethyl diazoacetate (EDA) by EPR spectroscopy and ESI mass spectrometry in an attempt to detect and characterize the putative Co^{II}(por)(CHCOOR) 'carbene' species. Detection of this species with EPR in combination with complementary DFT calculations should allow us to characterize their electronic structure in detail. Quite remarkably, despite the proposed unusual carbene radical character of these Co^{II}(por)(CHCOOR) species,[4a,16,17] their detection with EPR spectroscopy has not been reported.

Hence, in an attempt to investigate the electronic structure of the elusive carbene adducts, we investigated the reaction of the porphyrin complexes Co(TPP) and Co(3,5-Di^{t}Bu-ChenPhyrin)[4b] with EDA by EPR spectroscopy (Figure 2. Both these complexes are active catalysts for olefin cyclopropanation, but Co(3,5-Di^{t}Bu-ChenPhyrin) was shown to be much more active and selective.[4]

A solution of Co(TPP) in toluene at 40 K gave exactly the same EPR spectrum as reported previously by Van Doorslaer and Schweiger.[24] Quite remarkably, addition of 4 equiv of EDA to the toluene solution at RT led to instant and complete

(14) Related bridging carbene porphyrin complexes were also crystallographically characterized. Nickel: (a) Chevrier, B.; Weiss, R. *J. Am. Chem. Soc.* **1976**, *98*, 2985–2990 Ruthenium: (b) Seyler, J. W.; Safford, L. K.; Fanwick, P. E.; Leidner, C. R. *Inorg. Chem.* **1992**, *31*, 1545–1547. Iron with a bridging vinylidene species: (c) Chevrier, B.; Weiss, R.; Lange, M.; Chottard, J.-C.; Mansuy, B. *J. Am. Chem. Soc.* **1981**, *103*, 2899–2901. (d) Latos-Grazynski, L.; Cheng, R.-J.; La Mar, G. N.; Balch, A. L. *J. Am. Chem. Soc.* **1981**, *103*, 4270–4272. (e) Olmstead, M. M.; Cheng, R.-J.; Balch, A. L. *Inorg. Chem.* **1982**, *21*, 4143–4148.

(15) For Fe(por)(Cl)-nitrene complexes the formation of terminal vs bridging nitrenes seems to be dependent on the electronic properties of the nitrene ligand: (a) Mahy, J.-P.; Battioni, P.; Mansuy, D.; Fischer, J.; Weiss, R.; Mispelter, J.; Morgenstern-Badarau, I.; Gans, P. *J. Am. Chem. Soc.* **1984**, *106*, 1699–1706. (b) Mahy, J.-P.; Battioni, P.; Bedi, G.; Mansuy, D.; Fischer, J.; Weiss, R.; Morgenstern-Badarau, I. *Inorg. Chem.* **1988**, *27*, 353–359.

(16) Iwakura, I.; Tanaka, H.; Ikeno, T.; Yamada, T. *Chem. Lett.* **2004**, *33*, 140–141.

(17) Ikeno, T.; Iwakura, I.; Yamada, T. *J. Am. Chem. Soc.* **2002**, *124*, 15152–15153.

(18) (a) de Bruin, B.; Peters, T. P. J.; Thewissen, S.; Blok, A. N. J.; Wilting, J. B. M.; de Gelder, R.; Smits, J. M. M.; Gal, A. W. *Angew. Chem., Int. Ed.* **2002**, *41*, 2135–2138. (b) Hetterscheid, D. G. H.; Bens, M.; de Bruin, B. *Dalton Trans.* **2005**, *5*, 979–984. (c) Hetterscheid, D. G. H.; de Bruin, B.; Smits, J. M. M.; Gal, A. W. *Organometallics.* **2003**, *22*, 3022–3024. (d) Hetterscheid, D. G. H.; Smits, J. M. M.; de Bruin, B. *Organometallics.* **2004**, *23*, 4236–4246. (e) Hetterscheid, D. G. H.; Klop, M.; Kicken, R. J. N. A. M.; Smits, J. M. M.; Reijerse, E. J.; de Bruin, B. *Chem.—Eur. J.* **2007**, *13*, 3386–3405. (f) Hetterscheid, D. G. H.; Smits, J. M. M.; de Bruin, B. *Organometallics.* **2004**, *23*, 4236–4246.

(19) Dzik, W. I.; Reek, J. N. H.; de Bruin, B. *Chem.—Eur. J.* **2008**, *14*, 7594–7599.

(20) For detailed overviews of open-shell reactivity in open-shell group 8 organometallic chemistry, including other examples of redox noninnocent ligands, see: (a) de Bruin, B.; Hetterscheid, D. G. H.; Koekkoek, A. J. J.; Grutzmacher, H. *Prog. Inorg. Chem.* **2007**, *55*, 247–354. (b) de Bruin, B.; Hetterscheid, D. G. H. *Eur. J. Inorg. Chem.* **2007**, *2*, 211–230.

(21) Fantauzzi, S.; Gallo, E.; Rose, E.; Raoul, N.; Caselli, A.; Issa, S.; Ragaini, F.; Cenini, S. *Organometallics* **2008**, *27*, 6143–6151.

(22) Related Rh^{II}(TMP) systems bind TEMPO reversibly ($K_{eq} \approx 10^4$) but undergo irreversible hydrogen atom and methyl group abstraction reactions from TEMPO at higher temperatures: Chan, K. S.; Li, X. Z.; Dzik, W. I.; de Bruin, B. *J. Am. Chem. Soc.* **2008**, *130*, 2051–2061.

(23) Irreversible binding of TEMPO to related Ir^{II} species to form diamagnetic TEMPO adducts has been reported: Hetterscheid, D. G. H.; Kaiser, J.; Reijerse, E.; Peters, T. P. J.; Thewissen, S.; Blok, A. N. J.; Smits, J. M. M.; de Gelder, R.; de Bruin, B. *J. Am. Chem. Soc.* **2005**, *127*, 1895–1905.

(24) Van Doorslaer, S.; Schweiger, A. *Phys. Chem. Chem. Phys.* **2001**, *3*, 159–166.

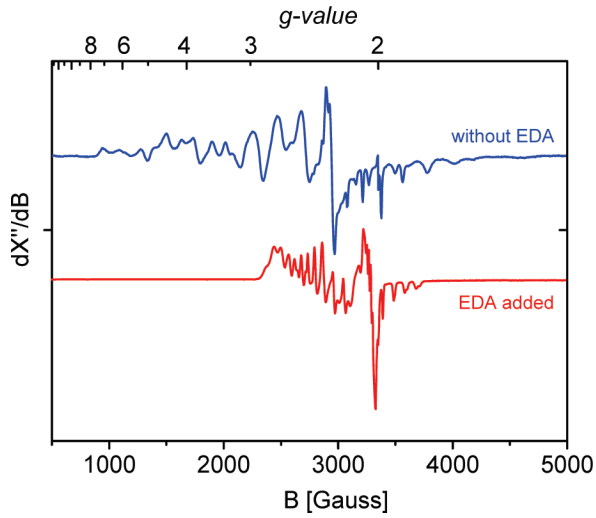

Figure 3. X-band EPR spectrum of [Co(3,5-Di^{t}Bu-ChenPhyrin)] before (top) and after (bottom) addition of EDA. Spectra were recorded in frozen toluene at 40 K.

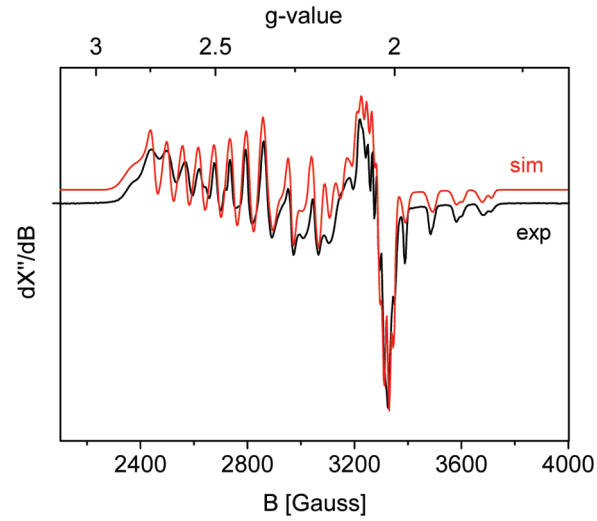

Figure 4. Experimental and simulated X-band EPR spectra of the species formed upon addition of EDA to a toluene solution of Co(3,5-Di^{t}Bu-ChenPhyrin). Experimental conditions: T = 40 K, frequency = 9.377430 GHz, modulation amplitude = 5 gauss, power = 2 mW.

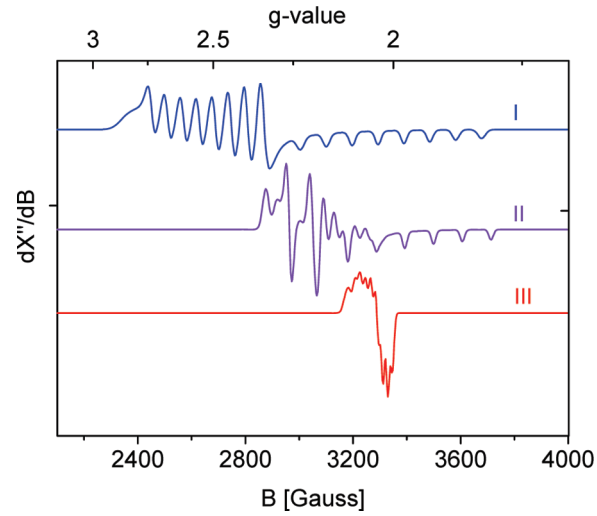

Figure 5. Individual components **I**, **II**, and **III** contributing to the EPR spectrum shown in Figure 4.

disappearance of the EPR signals (measured in the range of 5−70 K). Although we cannot exclude that some diamagnetic material was being formed in this reaction (e.g. formation of Co^{III}(TPP)(CH_2COOEt) by hydrogen atom abstraction[7]), this does not seem to be the main reason for the EPR silence, considering the clear observation of [Co(TPP)(CHCOOEt)]$^+$ species representing the dominant signals in the ESI-MS spectrum of the same batch (*vide infra*). This was confirmed by measuring ^{1}H NMR spectra of Co(TPP) directly after addition of 4 equiv of EDA in [D_6]-benzene, which show only the presence of paramagnetically broadened Co(TPP)-derived signals, free EDA, diethyl maleate, and minute amounts of the previously observed diamagnetic species, Co^{III}(TPP)(CH_2-COOEt), in agreement with previous observations.[7] Hence, it seems that the Co(TPP)(CHCOOEt) radical species (irrespective of its exact structure) is EPR silent. The EPR silence can perhaps be explained by the presence of one or more exited states with energies close to the ground state causing rapid electron spin relaxation, in analogy with arguments proposed to explain the EPR silence of Ir^{II}(por) species.[25] However, the exact reason for the EPR silence of Co(TPP) samples in the presence of EDA is presently not clear and contrasts markedly with the results obtained with Co^{II}(3,5-Di^{t}Bu-ChenPhyrin) described below. Co(3,5-Di^{t}Bu-ChenPhyrin) shows a quite complex EPR spectrum in toluene at 40 K (Figure 3), indicating the presence of 2−3 paramagnetic cobalt species. EPR parameters of cobalt porphyrins are highly influenced by their ligand surroundings,[26] and it is known that Co(TPP) forms 1:1 and 1:2 adducts with toluene.[24] The approximately $g_{x,y} > 3$ and $g_z < 2$ and large A^{Co} values observed for Co(3,5-Di^{t}Bu-ChenPhyrin) in toluene are indicative of the expected square planar cobalt−porphyrin complex, and agree qualitatively with the reported data for Co(TPP) in toluene.

Addition of 4 equiv of EDA to the toluene solution at RT resulted in a considerable change of the spectrum (measured at 40 K), and revealed full conversion from a 4-coordinate complex to a mixture of axially coordinated Co(3,5-Di^{t}Bu-ChenPhyrin)(L) species. The spectrum could be simulated (Figures 3, 4, and 5) as a mixture of three species **I**, **II**, and **III** in a rough ratio of 5:1:0.8 (as derived from the spectral simulations).[27] The simulated EPR parameters of these species are listed in Table 1.

The g and A^{Co} values of species **II** are in the range of strong field carbon adducts (CO, isocyanides) of Co^{II} porphyrins,[28] whereas the signals of species **I** are indicative of coordination of a weak field ligand (comparable to H_2O).[24] Therefore, we assign the signals of species **I** to the EDA adduct Co^{II}(3,5-Di^{t}Bu-ChenPhyrin)(EDA), with EDA coordinated to cobalt either via its carbon, carbonyl or dinitrogen moiety. The signals of species **II** can be assigned to the '*bridging carbene*' species Co^{II}(3,5-Di^{t}Bu-ChenPhyrin)(CHCOOEt) (Figure 1, right).

Remarkably, the EPR parameters of the third species **III** are indicative for an 'organic radical' (Figure 5, bottom), but the

(25) Zhai, H.; Bunn, A.; Wayland, B. B. *Chem. Commun.* **2001**, 1294–1295.
(26) Ozarovski, A.; Lee, H. M.; Balch, A. L. *J. Am. Chem. Soc.* **2003**, *125*, 12606–12614.
(27) As the EPR experiments were performed by freeze-quenching the EPR tube in liquid N_2, the detected distribution of the species **II** and **III** does not necessarily reflect their equilibrium distribution.
(28) Wayland, B. B.; Sherry, A. E.; Bunn, A. G. *J. Am. Chem. Soc.* **1993**, *115*, 7675–7684.

Table 1. Experimental[a] and DFT Calculated[b] EPR Parameters[c]

	g_x	g_y	g_z	$A^{Co}{}_x$	$A^{Co}{}_y$	$A^{Co}{}_z$	$A^{H}{}_x$	.	$A^{H}{}_z$
I[a]	2.558	2.520	2.004	255	208	270	–	–	–
Co(TPP)(H_2O)[e]	2.505	2.505	2.014	265	265	315			
II[a]	2.228	2.120	2.005	110	115	300	–	–	–
Co(por)(CHCOOMe) 'bridging carbene'[b]	*2.332*	*2.183*	*2.070*	*−39*	*234*	*491*	–	–	–
III[a]	2.060	2.048	2.030	40	56	nr[d]	160	40	nr[d]
Co(por)(CHCOOMe) 'terminal carbene'[b]	*2.010*	*2.002*	*1.975*	*−67*	*−19*	*6*	*−77*	*−50*	*−13*

[a] Parameters from spectral simulations. [b] Orca, b3-lyp/TZVP. [c] Hyperfine couplings in MHz. [d] nr = not resolved. [e] Taken from reference 24.

simulations also reveal resolved hyperfine couplings with cobalt and a proton. We therefore assign these signals to the *'terminal carbene'* species Co^{II}(3,5-Di^{t}Bu-ChenPhyrin)(CHCOOEt), which we take as the first direct experimental evidence for its carbon-centered radical character (Figure 1, left). It thus seems that the 'bridging carbene' **II** and 'terminal carbene' **III** isomeric forms of Co^{II}(3,5-Di^{t}Bu-ChenPhyrin)(CHCOOEt) exist in dynamic equilibrium with each other in solution.[27]

The EPR parameters of the 'bridging carbene' species Co^{II}(por)(CHCOOMe) (**II**) and the 'terminal carbene' species Co^{II}(por)(CHCOOMe) (**III**) were also calculated with DFT methods, using the nonsubstituted porphyrin ring (por), and methyl esters (from MDA) instead of ethyl esters. The DFT data of these simplified models are in good qualitative agreement with the experimental data of species **II** and **III**, respectively (Table 1). DFT calculated EPR parameters of methyl diazoacetate (MDA) adducts of Co^{II}(por) do not agree at all with the experimental parameters of species **I**, but this is not surprising because it is known that classical DFT approaches do not perform well in predicting the EPR parameters of undistorted Co porphyrin systems.[29] However, the EPR parameters of species **I** most likely belong to an axial adduct with a weak field ligand, because its EPR parameters qualitatively agree with those reported for Co(TPP)(H_2O).[24]

The same reaction mixtures used for the above EPR investigations were also analyzed with electrospray ionization mass spectrometry (ESI-MS). The ESI-MS spectrum of Co(TPP) exposed to 4 equiv of EDA in toluene reveals a major signal corresponding to $[Co(TPP)(CHCOOEt)]^+$ (m/z = 757.20) along with very low-intensity signals corresponding to $[Co(TPP)]^+$ (m/z = 671.10) and $[Co(TPP)(CHCOOEt)_2]^+$ (m/z = 843.30).

Similar results were obtained for Co^{II}(3,5-Di^{t}Bu-ChenPhyrin). Major peaks of [Co(3,5-Di^{t}Bu-ChenPhyrin)(CHCOOEt)]$^+$ (m/z = 1425.7) were detected in both toluene and CD_2Cl_2. Peaks corresponding to the alkyl species [Co(3,5-Di^{t}Bu-ChenPhyrin)(CH_2COOEt)]$^+$ (m/z = 1426.7) in toluene and [Co(3,5-Di^{t}Bu-ChenPhyrin)(CHDCOOEt)]$^+$ (m/z = 1427.7) in CD_2Cl_2 were also observed. They are indicative for hydrogen atom abstraction from the solvent in agreement with the radical deactivation pathway of the Co(TPP)(CHCOOEt) carbene species reported by Cenini and co-workers.[7] The spectrum in CD_2Cl_2 revealed also a strong signal corresponding to [Co(3,5-Di^{t}Bu-ChenPhyrin)$(CHCOOEt)_2]^+$ (m/z = 1511.7). This signal was also present in toluene, but in lower intensity.

The observed 2:1 carbene:Co adducts likely have a comparable structure to that reported for $[Co^{III}(OEP)(CHCOOEt)_2]NO_3$ (OEP = octaethylporphyrin) (i.e., with two 'carbene' moieties bridging between the cobalt and pyrrole nitrogen atoms, and located on opposite sides of the porphyrin ring; see Figure 11, species **F′**).[12d] However, cyclopropanation of a pyrrole double bond, insertion of the carbene into a C−H bond or a Büchner ring expansion cannot be ruled out.[30]

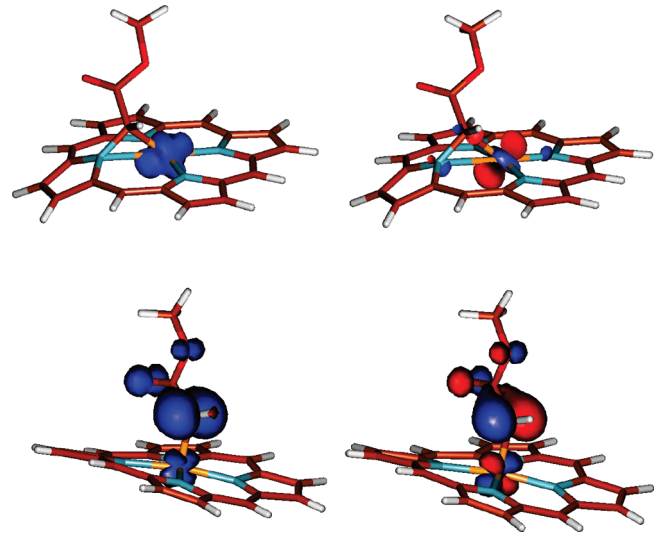

Figure 6. Spin density (left) and SOMO (right) plots of the DFT optimized 'bridging carbene' (top) and 'terminal carbene' (bottom) isomers of Co^{II}(por)(CHCOOMe).

2.2. Electronic Structures of the 'Terminal Carbene' and 'Bridging Carbene' Species. The singly occupied molecular orbitals (SOMO) and spin density plots of the 'bridging carbene' and 'terminal carbene' isomers of Co^{II}(por)(CHCOOMe) were calculated using DFT methods and are presented in Figure 6.

According to these calculations, the 'bridging carbene' complex is clearly a metal-centered radical, with its unpaired electron residing mainly in the cobalt $3d_{z^2}$ orbital, in good agreement with the measured EPR parameters (Table 1).

The spin distribution in the 'terminal carbene' complex is strikingly different. The unpaired electron resides mainly on the 'carbene' carbon, i.e. the α-carbon of the methyl 2-ylideneacetate moiety, and is slightly delocalized over the neighboring cobalt and oxygen atoms. This electronic structure agrees well with the EPR spectrum of **III**, which is indicative of an 'organic radical'. Hence, the 'terminal carbenes' are best described as carbon centered radicals (or 'carbene radicals') rather than true transition metal carbene moieties in the classic sense.

Species **II** and **III** represent an interesting example of equilibrium between two redox isomers. The 'bridging carbene'

(29) (a) Atanasov, M.; Daul, C. A.; Rohmer, M. M.; Venkatachalam, T. *Chem. Phys. Lett.* **2006**, *427*, 449–454. For a more general overview on the performance of DFT in predicting EPR parameters see: (b) Neese, F. *J. Biol. Inorg. Chem.* **2006**, *11*, 702–711. (c) Neese, F. *Coord. Chem. Rev.* **2009**, *253*, 526–563.

(30) Gomes, A. T. P. C.; Leão, R. A. C.; Alonso, C. M. A.; Neves, M. G. P. M. S.; Faustino, M. A. F.; Tomé, A. C.; Silva, A. M. S.; Pinheiro, S.; de Souza, M. C. B. V.; Ferreira, V. F.; Cavaleiro, J. A. S. *Helv. Chim. Acta* **2008**, *91*, 2270–2283.

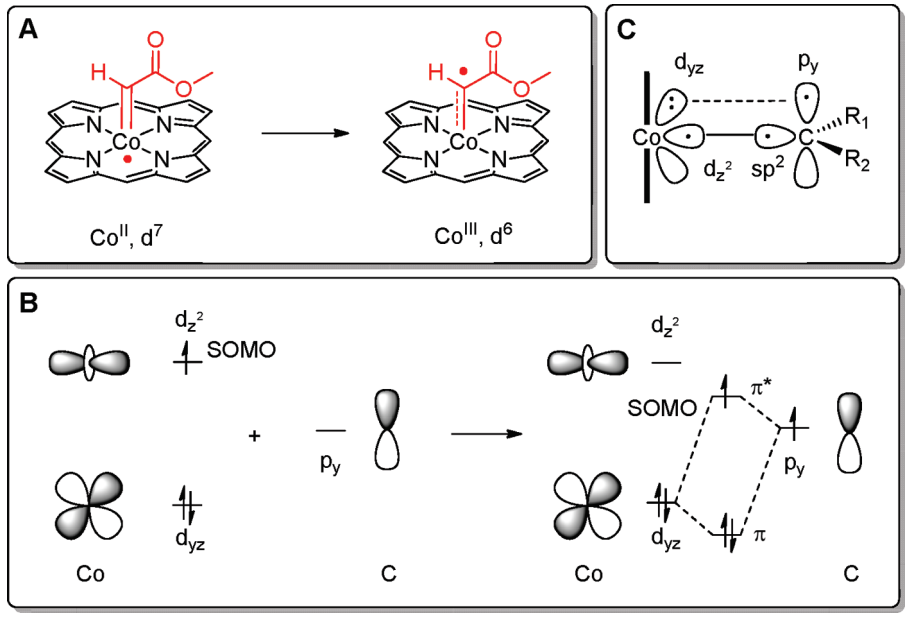

Figure 7. Redox noninnocent behavior of carbenes coordinated to open-shell Co^{II}(por) species explained by a simplified MO bonding scheme.

II is a d^7 Co^{II} complex, while the d^6 Co^{III} terminal carbene complex **III** has the unpaired electron located on the 'carbene ligand'. This is a situation somewhat similar to the recently reported dynamic interconversion between two [Rh(trop$_2$-PPh)(PPh$_3$)] electromers[31] or valence tautomers[32] of Co^{III}-(cateholato)−Co^{II}(semiquinato).[33]

Occupation of spin density on the 'carbene' carbon is not completely unexpected. The LUMO of an electrophilic Fischer-type carbene is carbon-centered and allows for one-electron reduction to a corresponding carbon-centered radical with external reducing agents.[34] Casey and co-workers showed that reduction of chromium pentacarbonyl alkoxyaryl complex by one electron led to a carbon-centered radical anion, persistent at −50 °C, as evidenced by EPR.[35] Since then, several other group 6 carbene radical anions have been reported to have nucleophilic carbon radical character and to undergo e.g. dimerization, coupling with electron-deficient alkenes and hydrogen atom abstraction reactions.[36] So clearly Fischer-type carbene ligands are redox noninnocent and *intramolecular* electron transfer from the electropositive metal center to the carbene moiety cannot be excluded as an alternative pathway for formation of 'carbene radicals'. This is exactly what happens for the 'terminal carbene' species Co^{II}(por)(CHCOOMe) (Figure 7A). A schematic representation of the relevant orbital interactions is shown in Figure 7. The interaction with the singlet :CHCOOMe moiety pushes the energy of the cobalt d$_{z^2}$ orbital above the energy of the antibonding MO constructed from the carbon p$_y$ orbital and cobalt d$_{yz}$ orbital, thus resulting in intramolecular electron transfer from cobalt to the carbene moiety (Figure 7A and B). Half filling of the Co−C π^* antibonding orbital thus substantially reduces the metal−carbon bond order. Hence, the 'carbene' species loses typical Fischer-type character, gains unusual radical reactivity, and becomes more nucleophilic. However, its open-shell radical character, putting discrete unpaired spin density on the 'carbene' carbon, is an important difference from any closed-shell Fischer- and Schrock-types of carbene descriptions.

Exactly the same electronic structure arises if the bonding is considered as a triplet carbene interacting with the Co^{II}(por) species (Figure 7C). Formation of a Co−C σ-bonding pair from the unpaired electrons in the cobalt d$_\sigma$ orbital and the triplet carbene sp^2 orbital leaves an unpaired electron in the p$_y$ orbital, effectively generating the same carbene radical ligand. 'Formal' oxidation state counting leads to a cobalt(III)−carbene anion radical in each case.

The radical character of the 'carbene' carbon atom of Co(por)(CHCOOR) species is likely responsible for the formation of the alkyl species Co^{III}(por)(CH$_2$COOEt) through hydrogen atom abstraction.[7] A similar behavior was observed for Rh^{II}(TMP) (TMP = tetramesitylporphinato) which reacts with diazo compounds to form Rh^{III}(TMP)(alkyl) species.[37] Recently, de Bruin and co-workers reported comparable redox noninnocent behavior of carbenes bound to paramagnetic •Ir^{II} species.[19,20] The resulting Ir^{III}(•CHR) 'carbene radicals' react with (Ir-coordinated) ethene to form new C−C bonds (or undergo similar hydrogen atom abstraction for more bulky 'carbenes').[19]

2.3. Mechanistic DFT Studies. Having established a clear picture of the (electronic) structure of the Co(por)(•CHCOOR) 'carbene radical' species in the previous sections, we next addressed their potential as intermediates in the catalytic cyclopropanation reactions with computational DFT methods.

2.3.1. Computational Methods. The BP86 functional is generally accurate in predicting the geometries of transition

(31) Puschmann, F. F.; Harmer, J.; Stein, D.; Rüegger.; de Bruin, B.; Grutzmacher, H. *Angew. Chem., Int. Ed.* **2010**, *49*, 385–389.
(32) For an excellent overview, see: Sato, O.; Tao, J.; Zhang, Y.-Z. *Angew. Chem., Int. Ed.* **2007**, *46*, 2152–2187.
(33) (a) Poneti, G.; Mannini, M.; Sorace, L.; Saintctavit, P.; Arrio, M.-A.; Otero, E.; Criginski Cezar, J.; Dei, A. *Angew. Chem., Int. Ed.* **2010**, *49*, 1954–1957. (b) Dapporto, P.; Dei, A.; Poneti, G.; Sorace, L. *Chem.—Eur. J.* **2008**, *14*, 10915–10918. (c) Beni, A.; Dei, A.; Laschi, S.; Rizzitano, M.; Sorace, L. *Chem.—Eur. J.* **2008**, *14*, 1804–1813.
(34) Block, T. F.; Fenske, R. F.; Casey, C. P. *J. Am. Chem. Soc.* **1976**, *98*, 441–443.
(35) Krusic, P. J.; Klabunde, U.; Casey, C. P.; Block, T. F. *J. Am. Chem. Soc.* **1976**, *98*, 2015–2018.
(36) For an excellent overview on one electron-activated (group 6) metal Fischer carbenes see: Sierra, M. A.; Gómez-Gallego, M.; Martínez-Álvarez, R. *Chem.—Eur. J.* **2007**, *13*, 736–744.
(37) Zhang, L.; Chan, K. S. *Organometallics* **2007**, *26*, 679–684.

metal complexes,[38] and has an excellent performance, especially for 3d metal compounds.[39] Extensive DFT computational studies of cobalt porphyrins and related cobalamin derivatives have illustrated that the observed Co−C bond dissociation enthalpies (BDE) and internuclear distances are best reproduced by the nonhybrid BP86. Hence, for reactions in which the making and breaking of cobalt−carbon bonds plays an important role, especially in cases where open-shell intermediates are involved, the use of the BP86 functional is preferred over B3LYP.[40] We have previously shown that the use of the BP86 functional gives accurate predictions of the thermodynamic energies and kinetic barriers associated with catalytic chain transfer[41] and degenerative radical exchange processes of radical polymerization reactions controlled by Co(por) complexes.[42] The Co−C bond should play an important role in predicting the energies and barriers for the Co(por)-catalyzed cyclopropanation reactions described in this paper. We therefore consistently used the nonhybrid BP86 functional in our studies.

Generally, Co^{II}(por) systems and their adducts Co^{II}(por)(L) have a low-spin d^7 doublet ($S = {}^1/_2$) ground state,[43] and related DFT calculations reported by Yamada and co-workers have shown that the contribution of higher spin states to the cyclopropanation mechanism in reactions mediated by Co(salen) models can be neglected[6b] (even at the hybrid B3LYP level, which is known to favor higher spin state stabilities[44]). Hence, all calculations were performed with complexes in their doublet ($S = {}^1/_2$) spin states. The reported free energies in kcal mol^{-1} are obtained from the calculated internal energies at the TZVP basis set on all atoms, adjusted for the zero-point energy, entropy, and approximately for the condensed phase reference volume (see Experimental Section). We used the nonfunctionalized cobalt porphyrin Co(por) as a smaller model of the experimental Co(TPP) complex. In addition we included some calculations using the Co(porAmide) model containing a 2-acetamidophenyl substituted porphyrinato ligand as a smaller model of the experimental Co(3,5-Di^{t}Bu-ChenPhyrin) system, in order to account for possible effects of hydrogen bonding interactions between the carbonyl moiety of MDA and the ligand amide functionalities (Figure 8).[4f]

2.3.2. Formation of the 'Carbene' Complexes from Co^{II}(por) and MDA. We first focused on the formation of the terminal and bridging 'carbene' species Co(por)(•CHCOOR) from MDA and the Co^{II}(por). Experimentally, cobalt complexes with amide functionalized porphyrins exhibited higher activities in alkene cyclopropanation reactions as compared to Co(TPP). In view of these higher activities, we also investigated the same reactions with the amide-functionalized Co^{II}(porAmide) model, in order to study the possible effect of hydrogen-bonding

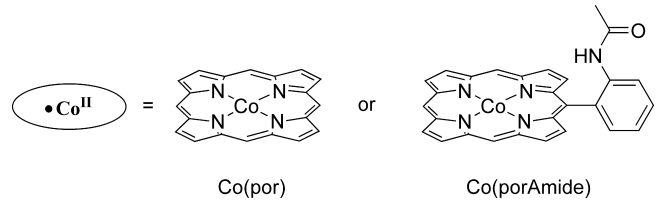

Figure 8. Cobalt porphyrin models used in the DFT studies.

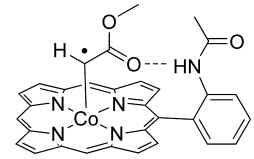

Figure 9. Relevant hydrogen-bonding interactions in formation and stabilization of the 'carbene' species.

interactions between the amide functionality of the porphyrin and the carbonyl group of the diazoacetate on the rate of 'carbene' formation (Figure 9).[4f]

The calculated free energies for the reaction of MDA with Co(por) and Co(porAmide) are plotted in Figure 10.

The DFT calculations predict the availability of three possible MDA adducts Co^{II}(por)(MDA) from the Co^{II}(por) species **A** and MDA. The carbonyl O-bound adduct **B″** has the lowest energy, +4.8 kcal mol^{-1} uphill relative to **A**. The nitrogen-bound adduct **B′** is slightly higher in energy (+5.1 kcal mol^{-1}), and the carbon-bound adduct **B** has the highest energy (+8.9 kcal mol^{-1}). The carbon-bound adduct **B**[45] is, however, the only productive adduct, allowing the elimination of dinitrogen (N_2) to form the radical carbene species **C** via a relatively high barrier transition state **TS1** (+13.1 kcal mol^{-1} from **B**; +22.0 kcal mol^{-1} from **A**). This barrier is in good qualitative agreement with the relatively slow cyclopropanation kinetics of Co(TPP).[4a,7,46]

Once formed, the 'terminal carbene' species **C** readily collapses to form the somewhat more stable 'bridging carbene' species **C′**. The energy difference between these species is, however, not large (1.5 kcal mol^{-1}), suggesting that these species should be in dynamic equilibrium with each other. The DFT calculations are in good agreement with the results from the EPR measurements. The calculated barriers for converting **C** into **C′** (12.9 kcal mol^{-1}) and *vice versa* (14.4 kcal mol^{-1}) are low enough to establish a fast equilibrium at room temperature.

Hydrogen bonding between the amide N−H of Co(porAmide) and the carbonyl oxygen of MDA (Figure 9) lowers the energy of the carbon-bound adduct **B**, the transition state **TS1**, and the carbene radical **C** by 1.7, 3.1, and 3.1 kcal mol^{-1}, respectively. The overall barrier for formation of species **C** from Co(porAmide) and MDA is lowered to 18.9 kcal mol^{-1}, in good qualitative agreement with the experimentally observed faster cyclopropanation reactions with amide-functionalized cobalt porphyrins.[4b−f,46]

Recently, a mechanistic study on Os(TTP)-mediated cyclopropanation indicated that the *trans* bis-'terminal carbene' osmium species is the active catalyst (TTP = 5,10,15,20-tetra-*p*-tolylporphyrinato).[47] Hence, we also investigated the pos-

(38) Schultz, N. E.; Zhao, Y.; Truhlar, D. G. *J. Phys. Chem. A* **2005**, *109*, 11127–11143.
(39) Furche, F.; Perdew, J. P. *J. Chem. Phys.* **2006**, *124*, 044103.
(40) See for example: (a) Jensen, K. P.; Ryde, U. *J. Phys. Chem. A* **2003**, *107*, 7539–7545. (b) Kuta, J.; Potchkovskii, S.; Zgierski, M. Z.; Kozlowski, P. M. *J. Comput. Chem.* **2006**, *27*, 1429–1437. (c) Qi, X. J.; Li, Z.; Fu, Y.; Guo, Q. X.; Liu, L. *Organometallics* **2008**, *27*, 2688–2698.
(41) de Bruin, B.; Dzik, W. I.; Li, S.; Wayland, B. B. *Chem.—Eur. J.* **2009**, *15*, 4312–4320.
(42) Li, S.; de Bruin, B.; Peng, C.-H.; Fryd, M.; Wayland, B. B. *J. Am. Chem. Soc.* **2008**, *130*, 13373–13381.
(43) Walker, F. A. In *The Porphyrin Handbook*; Kadish, K. M., Smith, K. M., Guilard, R., Eds.; Academic Press: New York, 2000; Vol. 5, pp 160−163,
(44) (a) Harvey, J. N.; Poli, R.; Smith, K. M. *Coord. Chem. Rev.* **2003**, *238−239*, 374–361. (b) Harvey, J. N. *Annu. Rep. Prog. Chem., Sect. C.* **2006**, *102*, 203–226, and references therein.
(45) A related C-bound EDA adduct of Rh^{III}(por)(I) has been detected at low temperature: Maxwell, J. L.; Brown, K. C.; Bartley, D. W.; Kodadek, T. *Science* **1992**, *256*, 1544–1547.
(46) Reliable experimental energy barriers are not available.
(47) Hamaker, C. G.; Djukic, J.-P.; Smith, D. A.; Woo, L. K. *Organometallics* **2001**, *20*, 5189–5199.

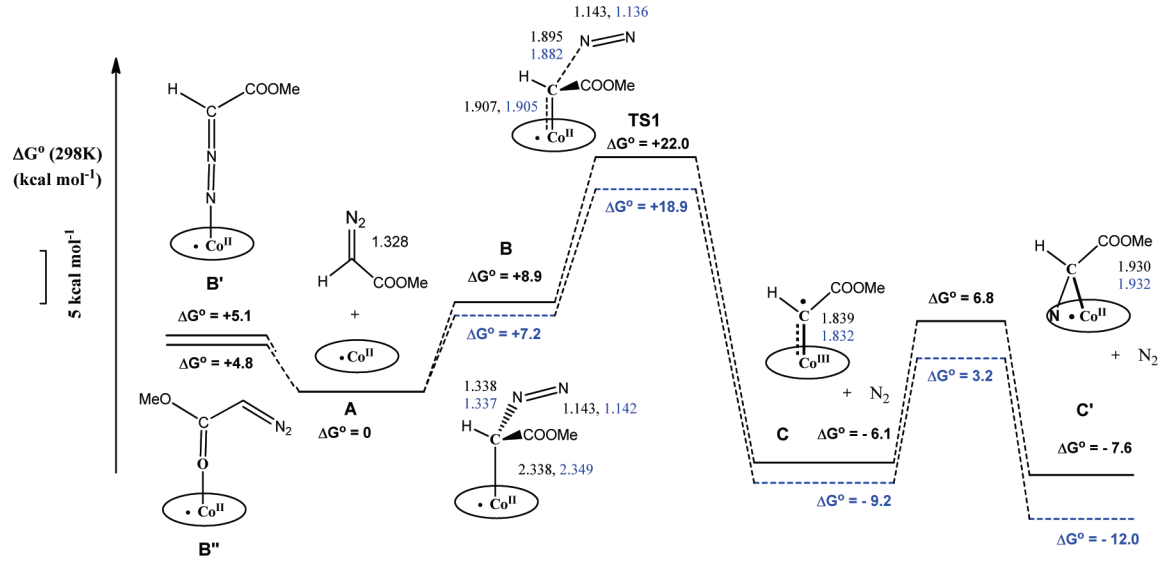

Figure 10. Free energy changes for the reaction of EDA with Co^{II}(por) (black) and with Co^{II}(porAmide) involving hydrogen bonding of the carbonyl group with the amide moiety (dashed blue). Selected bond distances (Å) are presented as well.

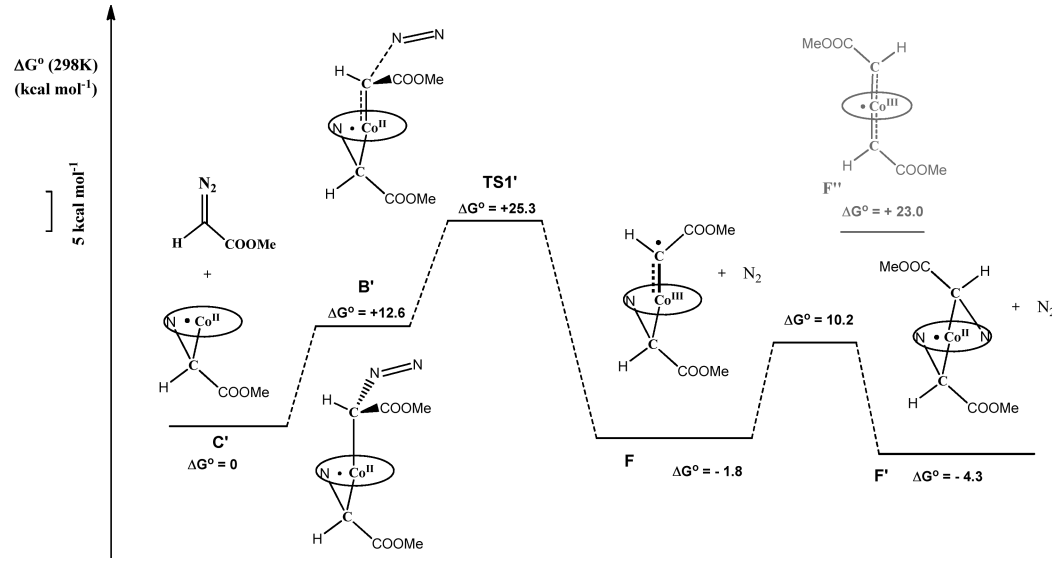

Figure 11. Reaction of MDA with 'bridging carbene' species **C′**.

sibility of formation of analogous cobalt bis-carbene species (see Figure 11). In the absence of olefin, slow formation of a bis-carbene species from the 'bridging carbene' Co^{II}(por)(CHCOOMe) species **C′** and MDA is both kinetically possible ($\Delta G^{\ddagger} = 25.3$ kcal mol^{-1}) and thermodynamically favorable ($\Delta G^{0} = -4.3$ kcal mol^{-1}), according to the DFT calculations. These calculations are in agreement with the detection of the species in the ESI-MS spectra in low intensities (*vide supra*). However, their formation under catalytic conditions in the presence of olefin is clearly kinetically disfavored from follow-up reactivity of **C′** with the olefinic substrate, which proceeds with much lower barriers (*vide infra*). Consequently, bis-carbene species Co^{II}(por)$(CHCOOR)_2$ should not play an (important) role under the catalytic conditions.

The *trans* bis-carbene species **F** (−1.8 kcal mol^{-1}) having one 'terminal carbene' and one 'bridging carbene' moiety can convert readily ($\Delta G^{\ddagger} = 12.0$ kcal mol^{-1}) to the somewhat more stable *trans* bis-'bridging carbene' species **F′** (−4.3 kcal mol^{-1}), according to the DFT calculations. Other *trans* bis-carbene isomers were found higher in energy, especially the *trans* bis-'terminal carbene' isomer **F″** (+27.3 kcal mol^{-1} relative to **F′**). Hence, the involvement of *trans* bis-'terminal carbene' species analogous to those proposed to be involved in Os(TPP)-mediated cyclopropanation can be safely excluded in the case of Co(por) systems.

2.3.3. Olefin Cyclopropanation via 'Carbene Radical' Addition to Olefins. We tried to find transition states for direct reactions of olefins with the MDA adduct **B**, Co^{II}(por)(MDA), in order to investigate the possibility of cyclopropanation proceeding via C−C coupling between the diazo adduct and olefin with simultaneous dinitrogen loss from the coordinated MDA moiety, as proposed by Cenini and co-workers.[7] Despite several attempts in approaching the problem with different constraint geometry variations, however, we were unable to find such transition states. Similarly, we were unable to find transition states for reaction of the 'bridging carbene' species **C′** with olefins. Therefore, we focused on the 'terminal carbene' species **C** as the remaining and most logical carbene transfer intermediate in the cyclopropanation mechanism. All free energies of the stationary points are referenced to the 'bridging carbene' species

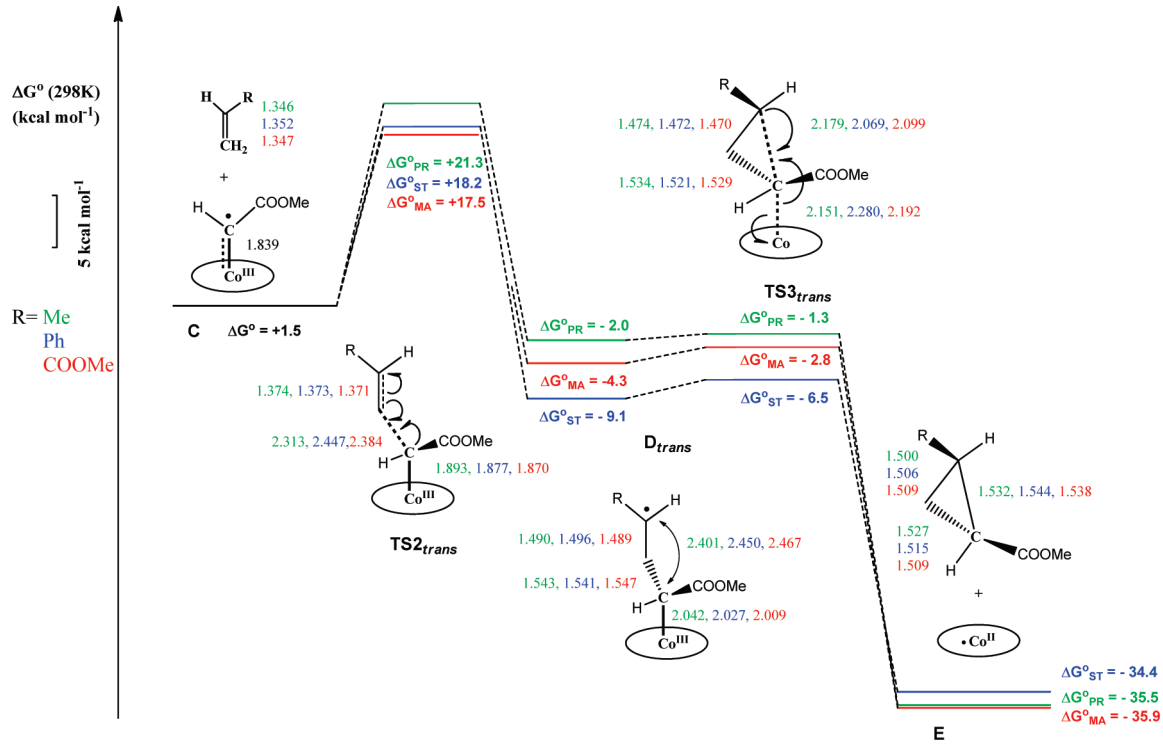

Figure 12. Computed pathways for *trans*-cyclopropanation of propene ($\Delta G°_{PR}$, green), styrene ($\Delta G°_{ST}$, blue) and methyl acrylate ($\Delta G°_{MA}$, red) mediated by Co(por)(CHCOOMe). Free energies in kcal mol^{-1} relative to the resting state 'bridging carbene' species **C′**.

C′, which should be a dormant state in the catalytic cyclopropanation cycle according to the DFT calculations.

We investigated the reaction of the 'terminal carbene' radical species **C** with three different types of alkenes: styrene, methyl acrylate, and propene. We chose propene as a model for aliphatic alkenes which generally do not form cyclopropanes effectively in Co^{II}(por)-catalyzed cyclopropanation with diazo compounds. Styrene is a benchmark substrate for cyclopropanation catalyzed by various transition metals, whereas methyl acrylate is an example of an electron-deficient olefin that is successfully cyclopropanated by Co^{II}(por) catalysts, but not by closed-shell Cu and Doyle-type Rh_2 catalysts.

The computed carbene transfer mechanism from the 'terminal carbene' species **C** clearly proceeds via a stepwise radical process, which contrasts with the concerted carbene transfer processes generally observed for closed-shell late transition metal catalysts in olefin cyclopropanation. The reaction involves the (irreversible) addition of the carbon-centered 'radical carbene' species **C** to the olefin, thus generating the Co(por)-(CHCOOMe−CH_2−CHR•) species **D** having its unpaired electron spin density primarily localized at the γ-carbon of the 'alkyl' moiety (see Figures 12 and 13). Formation of the species **D** is associated with relatively large barriers (**TS2**). These barriers are somewhat lower, but very comparable to the barrier (**TS1**) for formation of **C**, which is in excellent agreement with first-order kinetics in both [EDA] and [styrene] observed experimentally in the Co(TPP)-catalyzed styrene cyclopropanation.[7,48]

Once formed, the 'γ-alkyl radical' type species **D** readily collapse to form the corresponding cyclopropanes, regenerating the starting Co^{II}(por) species **A** to continue the catalytic cycle. This reaction can be described as a concerted radical type C−C bond formation with simultaneous homolysis of the Co−C bond. The overall computed carbene transfer steps are consistent with the expected bond length changes for the obtained two-step radical processes (see Figures 12 and 13).

The ring-closure reactions from **D** are very low-barrier processes (**TS3** < 2.6 kcal mol^{-1} in all cases). The barriers are actually so low that, apart from cyclopropanation, no other follow-up reactivity can be expected. For this reason, despite their carbon radical character and reactivity, the species **C** and **D** cannot, for example, initiate free radical polymerization reactions, which are associated with higher barriers.[49]

These **TS3** barriers are even lower than the barriers expected for C_β-C_γ bond rotation in these functionalized alkyls.[50] As a result, the diastereoselectivity of cyclopropanation is predetermined in the C−C bond-forming transition state **TS2**. In that sense, the computed two-step radical-type mechanism is not different from a concerted carbene transfer mechanism. We calculated pathways for formation of both the *trans*-cyclopropanes (Figure 12) and the *cis*-cyclopropanes (Figure 13) to gain some insight in the nature of the diastereoselectivity of the Co^{II}(por)-based catalytic systems. The geometries of the stationary points along the pathway for *cis*- and *trans*-cyclopropanation are very similar, and the differences are mainly energetic.

The two-step radical mechanism nicely explains the high activity of Co^{II}(por) catalysts in the cyclopropanation of electron-

(48) The **TS2** barrier is the most 'organic' reaction in the cyclopropanation cycle, with the least influence of cobalt. Hence, it is possible that the **TS2** barriers are somewhat underestimated by the use of the BP86 functional. The hybrid b3-lyp functional is probably better in predicting the barrier to **TS2** (see Supporting Information for somewhat higher **TS2** barriers) but is not suitable for all other reaction steps in the catalytic cycle.

(49) To initiate olefin radical polymerization, the barrier for cyclopropane ring closure (**TS3**) would have to be higher than 8 kcal mol^{-1}, i.e. higher than the activation energy for addition of olefinic monomers to a growing radical polymer chain: Fisher, H.; Radom, L. *Angew. Chem., Int. Ed.* **2001**, *40*, 1340–1371.

(50) The barrier for rotation of a C−C bond in propane is ∼3 kcal/mol, and we use it as the lower limit of the expected energy of rotation of the C_β−C_γ bond in species **D**. Carey, F. A.; Sundberg, R. J. *Advanced Organic Chemistry, Part A: Structure and Mechanisms*, 5th ed.; Springer: New York, 2007; p 142.

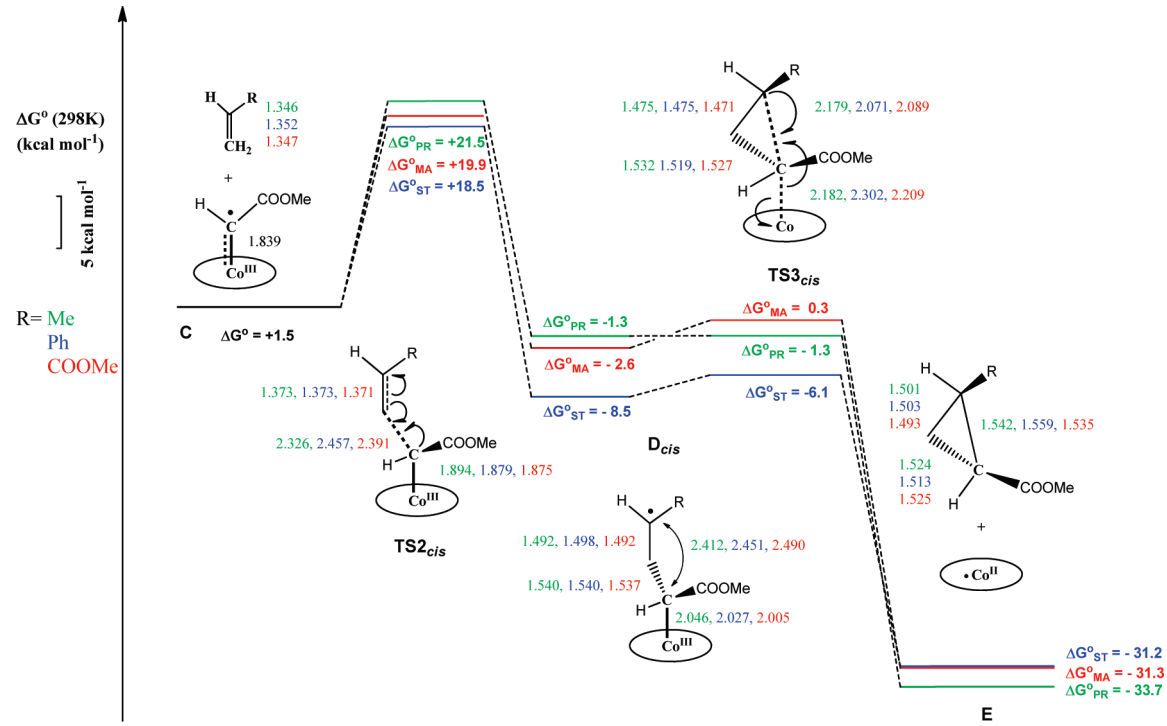

Figure 13. Computed pathways for *cis*-cyclopropanation of propene (ΔG°_{PR}, green), styrene (ΔG°_{ST}, blue), and methyl acrylate (ΔG°_{MA}, red). Free energies in kcal mol^{-1} relative to the resting state 'bridging carbene' species **C′**.

deficient olefins such as methyl acrylate, and their poor performance in cyclopropanation of electron-rich aliphatic alkenes. One-electron reduction of the redox noninnocent carbene ligand (by the Co^{II} center) should give the carbene carbon atom more nucleophilic character (Figure 7). Consequently, the relative energies of the transition states **TS2** should depend on the electrophilicity of the olefin (that is quantified by the global electrophilicity parameter, ω).[51] The ω values are 0.60 eV for propene, 1.13 eV for styrene, and 1.51 eV for methylacrylate[52] and correlate well with the calculated barriers. The relative stabilities of the species **D** are strongly dependent on the ability of the olefin R group (R = CH_3, Ph, COOMe) to stabilize the γ-carbon radicals. Reported radical stabilization energies[53] (RSE) are in the order: •CH(Me)CH_3 (−5.6 kcal mol^{-1}) < •CH(COOMe)CH_3 (−9.6 kcal mol^{-1}) < •CH(Ph)CH_3 (−14.3 kcal mol^{-1}) and are in good qualitative agreement with the relative stabilities of the species **D** (stabilization with Me < COOMe < Ph). These RSE values should partly influence **TS2** as well, hence explaining the relatively low **TS2** barrier for styrene (which cannot be explained by the ω value alone).

Due to steric reasons, the $\mathbf{TS2}_{cis}$ barriers for *cis*-cyclopropanation (Figure 13) are higher than the $\mathbf{TS2}_{trans}$ barriers for *trans*-cyclopropanation (Figure 12) in all cases. While the differences are very small for cyclopropanation reactions of propene and styrene, dipolar repulsion between the two carboxymethyl groups results in a quite substantial difference (2.4 kcal mol^{-1}) between the barriers for *cis*- and *trans*-cyclopropanation of methyl acrylate. This corresponds well with the high experimental *trans*:*cis* selectivity for cyclopropanation of methyl acrylate with EDA catalyzed by D_2-symmetric chiral porphyrin Co^{II} complexes.[4d]

Table 2. DFT Calculated Barriers for Olefin Addition to Radical Carbene **C** and Calculated and Experimental *trans*:*cis* Ratios at Room Temperature

olefin	ΔG_{trans}	ΔG_{cis}	*trans*:*cis*	expt.
methyl acrylate	17.5	19.9	98:02	99:01[a]
styrene	18.2	18.5	68:32	75:25[b]
propene	21.3	21.5	55:45	n.d.

[a] Co^{II}(3,5-Di^{t}Bu-ChenPhyrin), ref 4d. [b] Co^{II}(TPP), ref 4a.

The calculated *trans*:*cis* ratios for cyclopropanation of methyl acrylate, styrene and propene using the Co(por) catalyst are shown in Table 2. The calculated values are in excellent agreement with the available experimental data. The high *trans*:*cis* ratio obtained in cyclopropanation of methyl acrylate mediated by Co^{II}(3,5-Di^{t}Bu-ChenPhyrin) therefore seems to be general for Co^{II}(por) systems, and does not seem to be caused by its porphyrin steric bulk.

2.3.4. Suppression of Side-Product Formation by 'Carbene Dimerization'. One of the advantages of using Co^{II}(por) catalysts for cyclopropanation is their markedly suppressed 'carbene' dimerization activity under the practical catalytic conditions. Dimerization of diazo compounds to fumarates and maleates is the main side reaction in cyclopropanation mediated by most other catalysts (e.g., closed-shell Cu and Doyle-type Rh_2 catalysts). To suppress this common side reaction, slow addition of the diazo compound to the reaction mixture and/or use of excess olefins is usually required. In the case of the Co^{II}(por)-based systems, these precautionary procedures are not necessary as only trace amounts of carbene dimerization products are generally formed under the catalytic conditions.[4,7] In the absence of olefins, Co^{II}(por) catalysts do mediate slow carbene dimerization from the diazo substrates. This leads almost exclusively to the formation of maleates; apparently formation

(51) Parr, R. G.; von Szentpály, L.; Liu, S. B. *J. Am. Chem. Soc.* **1999**, *121*, 1922–1924.
(52) (a) Das, T. K.; Banerjee, M. *J. Phys. Org. Chem.* **2010**, *23*, 148–155. (b) Domingo, L. R.; Pérez, P.; Contreras, R. *Tetrahedron* **2004**, *60*, 6585–6591.
(53) Zipse, H. *Top. Curr. Chem.* **2006**, *263*, 163–189, and references therein.

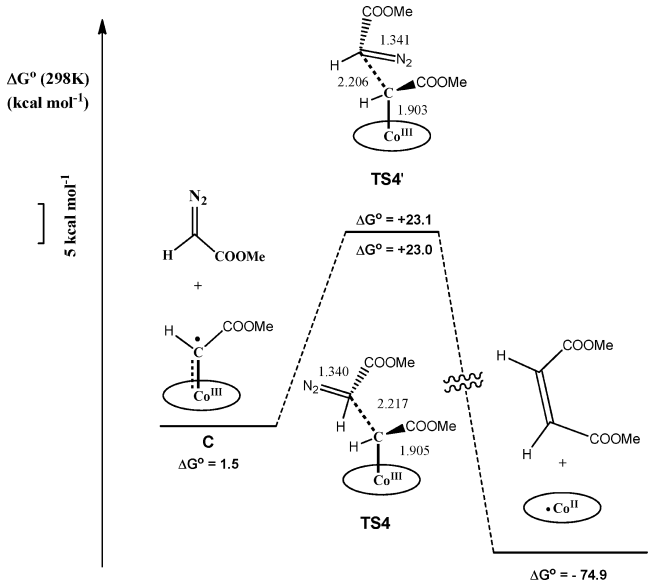

Figure 14. Formation of dimethyl maleate by dimerization of methyl diazoacetate.

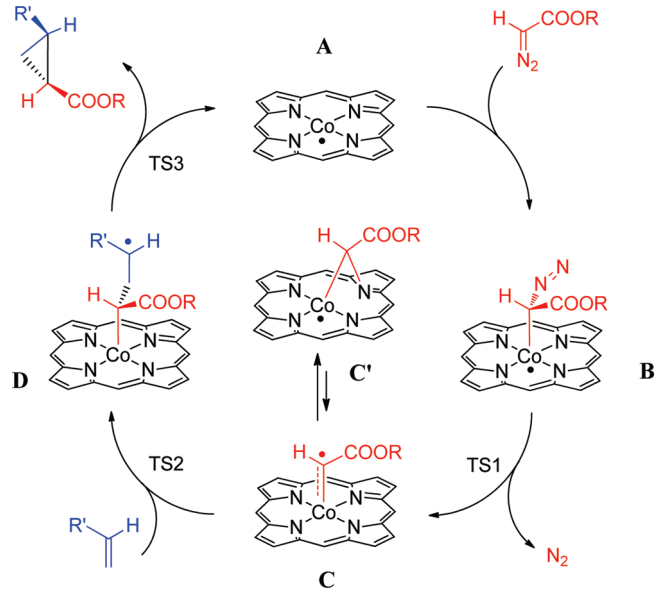

Figure 15. Catalytic cycle for Co(por)-catalyzed cyclopropanation of olefins.

of the thermodynamically favored fumarates is kinetically suppressed. We investigated these phenomena computationally to get some insight in the reasons behind the low dimerization activity and high maleate selectivity of Co^{II}(por)-based catalytic systems.

The calculated pathway for dimerization of MDA reveals two similar and relatively high-energy transition states **TS4** (23.0 kcal mol^{-1}) and **TS4′** (23.1 kcal mol^{-1}) for C−C bond formation between the 'terminal carbene' species **C** and MDA (see Figure 14 and Figure S8 in the Supporting Information). These reactions are followed by loss of dinitrogen from the diazo compound with simultaneous formation of dimethyl maleate in both cases. Formation of the kinetic product dimethyl maleate instead of the thermodynamically more stable dimethyl fumarate is a result of the steric influence between the porphyrin ring and the attacking diazoacetate (see Figure 14 and Figure S8 in Supporting Information). We were unable to find a transition state for formation of dimethyl fumarate. Since the calculated barrier for dimer formation is higher than the barriers for radical addition of **C** to methyl acrylate or styrene (<20 kcal mol^{-1}), carbene dimerization is expected to be suppressed, which is in good agreement with experimental observations under the catalytic conditions (i.e. in the presence of olefin).

3. Summary and Conclusions

On the basis of the results from the combined experimental (EPR and ESI-MS measurements) and computational (DFT calculations) studies, a catalytic cycle for Co^{II}(por)-mediated cyclopropanation of olefins is proposed to involve several unusual key intermediates as summarized in Figure 15.

The reaction proceeds via an unprecedented stepwise radical addition−substitution pathway, in which the redox noninnocent behavior of the terminal carbene ligand in intermediate **C** plays a key role (Figure 15). The Co^{II}(por) catalyst **A** reacts with the diazoester compound to form a transient adduct **B**, which loses dinitrogen in a rate-limiting step (**TS1**) to form the 'terminal carbene' intermediate **C**. The 'terminal carbene' **C** exists in equilibrium with the somewhat more stable 'bridging carbene' **C′**. Both **C** and **C′** species were detected experimentally from the reaction mixture of Co^{II}(3,5-Di^{t}Bu-ChenPhyrin) with EDA by EPR spectroscopy. The electronic structure of **C** is noteworthy. The species is a carbon-centered radical and is best described as a one-electron-reduced Fischer-type carbene. These results clearly underline the general importance of redox noninnocent ligands[54] and represent a rare example of the involvement of a ligand radical in organometallic catalysis.[19,20]

The 'bridging carbene' species **C′** is not capable of carbene transfer to the olefin and appears to be a dormant state in the catalytic cycle. The cobalt-centered radical **C′** has to transform back to the carbon-centered radical **C** to allow carbene transfer to the olefin. This proceeds via radical addition of the 'carbene radical' **C** to the C═C double bond of the olefin to form a γ-alkyl radical intermediate **D**. The intermediates **D** then readily collapse in almost barrierless ring-closure reactions (**TS3**) to form the cyclopropanes.

Addition of the 'terminal carbene' **C** to the olefin (**TS2**) proceeds with comparable barriers as its formation (**TS1**), thus explaining first-order kinetics in both substrates and the catalyst. Formation of **C** can be accelerated by stabilization of **C** and **TS1** via hydrogen bonding. Calculated barriers for Co^{II}(por)-mediated carbene dimerization are higher than the highest barriers for the olefin cyclopropanation, thus explaining the suppression of carbene dimerization under catalytic conditions.

The proposed radical-type mechanism (Figure 15) agrees well with all available mechanistic and kinetic information and readily explains the excellent performance of Co^{II}(por)-based systems in the cyclopropanation of electron-deficient olefins. The new insights obtained from these studies should shed light on how to address further selectivity issues in catalytic cyclopropanation and will aid future development of new catalytic systems for remaining difficult substrates. Furthermore, these mechanistic insights may lead to the development of new types of radical ring-closure processes by Co^{II}(por) catalysts (e.g.,

(54) Chirik, P. J.; Wieghardt, K. *Science* **2010**, *327*, 794–795.

formation of five-membered rings from properly designed 1,4-dienes and carbene sources).

Experimental Section

EPR and ESI-MS. Sample Preparation. Toluene was distilled under nitrogen from sodium wire; CD_2Cl_2 was degassed using pump−freeze−thaw method and dried over 4 Å molecular sieves. Co(3,5-Di^{t}Bu-ChenPhyrin)[4b] and Co(TPP)[55] were prepared according to published procedures. They were dissolved in toluene ($c_{Co(ChenPhyrin)} = 2.7 \times 10^{-3}$ M; $c_{Co(TPP)} = 10^{-4}$ M) or CD_2Cl_2 ($c_{Co(ChenPhyrin)} = 5.4 \times 10^{-3}$ M) and each solution was transferred into a Teflon-valved EPR tube in a N_2-filled glovebox, and their CW X-band EPR spectra were recorded. Co(TPP) gave exactly the same spectrum as reported by Van Doorslaer and Schweiger.[24] Next, 4 equiv of EDA were added under N_2 atmosphere, and the samples were shaken for 30−40 s and subsequently frozen in liquid nitrogen. Experimental X-band EPR spectra of these mixtures were recorded on a Bruker EMX spectrometer equipped with a He temperature-control cryostat system (Oxford Instruments) located in Nijmegen. The spectra were simulated by iteration of the anisotropic g values, (super)hyperfine coupling constants, and line widths. We thank Prof. F. Neese for a copy of his EPR simulation program. After 24 h, the samples were diluted with MeOH to the approximately concentration of 10^{-5} M, and their ESI-MS spectra were recorded. ESI-MS measurements were performed on a Shimadzu LCMS-2010A liquid chromatograph mass spectrometer by direct injection of the diluted sample to the ESI probe.

DFT. Geometry optimizations were carried out with the Turbomole program package[56] coupled to the PQS Baker optimizer[57] at the ri-DFT level using the BP86[58] functional and the resolution-of-identity (ri) method.[59] We used the SV(P) basis set[60] for the geometry optimizations of all stationary points. All minima (no imaginary frequencies) and transition states (one imaginary frequency) were characterized by numerically calculating the Hessian matrix. ZPE and gas-phase thermal corrections (entropy and enthalpy, 298 K, 1 bar) from these analyses were calculated. Improved energies were obtained with single point calculations at DFT/BP86 level using the Turbomole def-TZVP basis set.[61] Estimated condensed phase (1 L mol^{-1}) free energies, entropies and enthalpies were obtained from these data by neglecting the enthalpy RT term and subsequent correction for the condensed phase reference volume $S_{CP} = S_{GP} + R \ln(1/24.5)$. Selected single-point calculations at the b3-lyp,[62] def-TZVP level are reported in the Supporting Information. Calculated EPR spectra were obtained with Orca[63] at the DFT, b3-lyp,[62] TZVP[61] level, using the Turbomole optimized geometries.

Acknowledgment. The work was financially supported by The Netherlands Organization for Scientific Research - Chemical Sciences (NWO-CW VIDI Project 700.55.426; B.d.B.), the European Research Counsel (Grant Agreement 202886; B.d.B.), the University of Amsterdam (B.d.B.), American Chemical Society (44286-AC1; X.P.Z.), the National Science Foundation (CAREER Award: CHE-0711024; X.P.Z.), and the University of South Florida (Startup Funds; X.P.Z.).

Supporting Information Available: ESI-MS data of the reaction products formed upon addition of EDA to Co(TPP) and Co(3,5-Di^{t}Bu-ChenPhyrin); DFT optimized geometries, SOMO and spin density plots of species *trans*-**D**; Tables containing ΔE, ΔE_{ZPE}, ΔG, ΔH and ΔS values of all DFT optimized geometries; free energies for olefin cyclopropanation at the b3-lyp, def-TZVP level; computed IR CO stretching frequencies. This material is free of charge via the Internet at http://pubs.acs.org.

JA103768R

(55) Sugimoto, H.; Kuroda, K. *Macromolecules* **2008**, *41*, 312–317.
(56) Ahlrichs, R.; *Turbomole Version 5*; Theoretical Chemistry Group, University of Karlsruhe. Karlsruhe, Germany, 2002.
(57) *PQS*, version 2.4; Parallel Quantum Solutions: Fayetteville, AR, 2001. The Baker optimizer is available separately from PQS upon request. Baker, J. *J. Comput. Chem.* **1986**, *7*, 385–395.
(58) (a) Becke, A. D. *Phys. Rev. A* **1988**, *38*, 3098–3100. (b) Perdew, J. P. *Phys. Rev. B* **1986**, *33*, 8822–8824.
(59) Sierka, M.; Hogekamp, A.; Ahlrichs, R. *J. Chem. Phys.* **2003**, *118*, 9136–9148.
(60) Schaefer, A.; Horn, H.; Ahlrichs, R. *J. Chem. Phys.* **1992**, *97*, 2571–2577.
(61) Eichkorn, K.; Weigend, F.; Treutler, O.; Ahlrichs, R. *Theor. Chem. Acc.* **1997**, *97*, 119–124.
(62) (a) Lee, C.; Yang, W.; Parr, R. G. *Phys. Rev. B* **1988**, *37*, 785–789. (b) Becke, A. D. *J. Chem. Phys.* **1993**, *98*, 1372–1377. (c) Becke, A. D. *J. Chem. Phys.* **1993**, *98*, 5648–5652. (d) Calculations were performed using the Turbomole functional "b3-lyp", which is not identical to the Gaussian "B3LYP" functional.
(63) Neese, F. *ORCA: An ab Initio, Density Functional and Semiempirical Program Package*, version 2.7.0; University of Bonn, Bonn, Germany, 2009.